ISSN 1023-1935, Russian Journal of Electrochemistry, 2016, Vol. 52, No. 1, pp. 78–82. © Pleiades Publishing, Ltd., 2016.
Original Russian Text © Yu.D. Gamburg, V.V. Zhulikov, B.F. Lyakhov, 2016, published in Elektrokhimiya, 2016, Vol. 52, No. 1, pp. 90–94.

Electrodeposition, Properties, and Composition of Rhenium–Nickel Alloys

Yu. D. Gamburg[z], V. V. Zhulikov, and B. F. Lyakhov

Frumkin Institute of Physical Chemistry and Electrochemistry, Russian Academy of Sciences, Leninskii pr. 31, Moscow, 119071 Russia

Received January 29, 2014

Abstract—The process of deposition of the Re–Ni alloy, its current efficiency, and the alloy composition are studied as a function of the current density and the solution temperature. The hydrogen content in the deposits, their surface morphology, internal structure, and properties as the cathodic material for HER are examined. It is assumed that besides the high rhenium content, the high catalytic activity of nickel–rhenium alloys is associated with the high degree of their structural disordering.

Keywords: electrodeposition, alloys, nickel–rhenium, structure, hydrogen in metals, electrocatalysis

DOI: 10.1134/S1023193515120058

INTRODUCTION

Rhenium pertains to metals the deposition of which from aqueous solutions is associated with many complications. For the most part, this is due to the low overpotential of hydrogen evolution from the rhenium surface. For this reason, the Re deposition proceeds with a low current efficiency (CE) and is accompanied by the absorption of considerable amounts of hydrogen. Moreover, the metal forms from the perrhenate ion ReO_4^- according to the rough scheme $ReO_4^- + 7e + 8H^+ = Re + 4H_2O$, which suggests that the electricity consumption per mass unit is very high and the process substantially depends on the solution acidity. The higher deposition rates can be achieved by codeposition of rhenium with cobalt or nickel. The literature data concerning these processes are relatively few and mostly pertain to codeposition of rhenium with cobalt. Thus, rhenium–nickel deposits were considered only in several publications [1–4] which discussed the current efficiency and the possible mechanism of this process under optimal conditions.

It was shown [5] that the addition of an insignificant amount (1 g/L) of potassium perrhenate to the standard nickel-plating solution containing boric acid (pH 4.6) made it possible to obtain nickel–rhenium deposits with the high CE but with the rhenium content below 16%. In a solution of the same composition but with the addition of citric acid (pH 2.3), the rhenium content in the deposits obtained at the cathodic current density $j_c = 20$ mA/cm^2 reached 70% and CE was 25%. As j_c increased to 150 mA/cm^2, CE increased to 60% but the rhenium content in the deposit fell down to 10%. The properties of synthesized deposits were also characterized by these authors as regards their chemical stability in water, acids, and alkalis. The alloy surface was bright, the coatings tended to exfoliate from the copper support. Under laboratory conditions, the brightness stayed for 3 months (under similar conditions, nickel electroplates darkened in 10 days and in 3 months became covered by a dense oxide film). Nickel–rhenium deposits proved to be resistant to the action of dilute acids (except for nitric) and alkalis. The electrolyte proposed in [6] contained 56 g/L of nickel sulfate hexahydrate, 10 g/L of potassium perrhenate, and 66 g/L of citric acid. The recommended deposition conditions: j_c 50 mA/cm^2, pH 4–8, electrolyte temperature 70°C. The deposits contained 78 wt % rhenium for CE 90%, demonstrated high hardness and good adhesion to the copper support.

The mechanism of rhenium codeposition with nickel was considered in [7], where it was shown that depolarization and polarization at the codeposition of nickel with rhenium are mainly determined by the variations in the M–H bond energy on the alloy surface with the alloy composition.

The later studies [8–10] discussed the possibility of increasing the alloy current efficiency and the rhenium content and also the possibility of synthesizing a catalytically active alloy by applying magnetic field.

Alloys Ni–Re are promising precisely due to their catalytic properties, because both rhenium and nickel demonstrate low overpotentials in the hydrogen evolution reaction (HER) and, hence, can accelerate certain processes of cathodic reduction.

The present study considers the process of Re–Ni alloy deposition, its current efficiency, the alloy composition depending on the current density and solution temperature and also the hydrogen content in deposits, their surface morphology, internal structure, and properties as the cathodic materials for HER.

[z] Corresponding author: gamb@list.ru (Yu.D. Gamburg).

EXPERIMENTAL

In preliminary experiments, we have found the following optimal solution composition: 77 g/L $NiSO_4$, 57.8 g/L $KReO_4$, and 9.6 g/L citric acid (0.5, 0.2, and 0.05 M, respectively). Solutions were prepared from distilled water and the following chemicals: $NiSO_4 \cdot 7H_2O$ (chemical degree of purity), $KReO_4$ (analytical degree of purity), citric acid (reagent degree of purity). The deposition was carried out in the temperature interval from 42 to 62°C, where temperatures of 56–60°C were the optimal. We used two types of cathodes: a common planar copper electrode and multipoint microcathodes [11]. For a planar cathode, the deposits represented foils adhered rather strongly to its surface. For microcathodes, the very high current densities could be reached, which allowed obtaining deposits in the form of disperse dendrite powders which detached from the surface and fell down to cell's bottom. Multipoint cathodes represented an assembly of wire ends with the diameter of 150 μm exposed to the surface of a perfluorated plastic cylinder with the diameter of 20 mm. The total working surface of such electrode was 0.007 cm^2; the working surface of planar electrodes was 2–4 cm^2. Preliminary experiments have shown that it is technologically more convenient to use a multipoint electrode made of a MGTF wire with the diameter of 150 μm. The cathode was assembled of 40 parallel wire segments with the length of 3 cm which were distributed over the spherical surface. To eliminate the mutual influence of their diffusion fields in solution, the distance between wire ends was 1.5–2 mm. When measuring polarization, the Luggin capillary orifice was placed in the center of the sphere of microelectrodes.

The deposition was carried out under galvanostatic conditions until the coating thickness of 10–15 μm was reached (for powder, until the total mass of the deposit was 15–20 mg) without solution agitation.

Studies of the cathodic polarization were carried out by means of the IPC-PRO potentiostat (Frumkin Institute of Physical Chemistry and Electrochemistry, RAS) in the potentiodynamic mode with the potential scan rate of 10 mV/s in a standard three-electrode cell with a silver/silver-chloride reference electrode. The Luggin capillary was brought close to the electrode surface at a distance of 1–1.5 mm. In the majority of measurements carried out on microcathodes, the current flowing through the cell did not exceed 10 mA. This is why the ohmic potential drop was left uncompensated. In experiments with planar electrodes, the ohmic component measurements by the method of potential decay and the corresponding corrections were made automatically. In the figures, the potential is shown with respect to the hydrogen electrode.

The hydrogen content in alloys was found by the method of vacuum extraction by the procedure described, e.g., in [12].

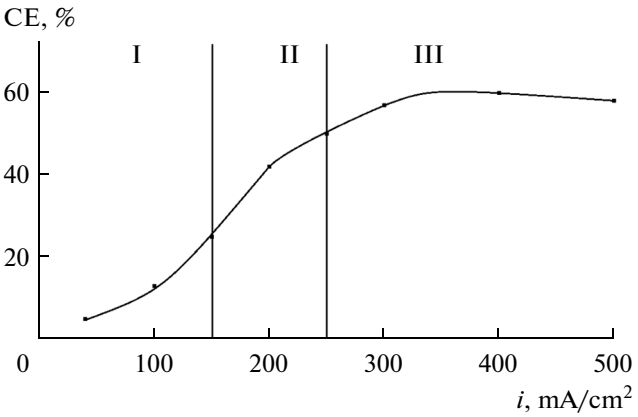

Fig. 1. Current efficiency of rhenium–nickel alloys as a function of the current density. Deposit type: (I) dense, (II) transition, (III) powders.

EXPERIMENTAL RESULTS

1. Current Efficiency and the Type of Deposits

Figure 1 shows the general dependences of the type of prepared deposits and the current efficiency on the current density. It can be seen that the region of synthesis of compact coatings corresponds to the current densities below 150 mA/cm^2; in this case, the current efficiency was 5–25%.

For the nickel–rhenium alloy, the extremely low CE was observed for current densities below 40 mA/cm^2. The dependence of CE on j_c resembles the dependence of the nickel content in the alloy on the current density. This may point to the high catalytic activity of nickel in the reduction of perrhenate ions, confirming the assumptions of several scientists [7, 13]. Correspondingly, these deposits had the high rhenium content and the hydrogen overpotential of rhenium was low. For current densities above 150 mA/cm^2, the limiting diffusion current with respect to nickel ions was reached and the high cathodic potential favored acceleration of the cathodic hydrogen evolution reaction.

The EC of the alloy considerably decreased with the decrease in pH.

2. Cathodic Polarization

Figure 2 shows the polarization curves for the deposition of the rhenium–nickel alloy. The alloy deposition proceeded with the lower overpotential as compared with individual nickel. This can be associated with the greater role of adsorbed hydrogen in the cathodic process and also with the catalytic effect of freshly deposited nickel on the process of perrhenate ion reduction.

Cyclic polarization curves measured on the surface of an alloy-covered nickel sample at the potential scan rate of 10 mV/s in the range from the open-circuit potential to –1 V demonstrated a considerable hyster-

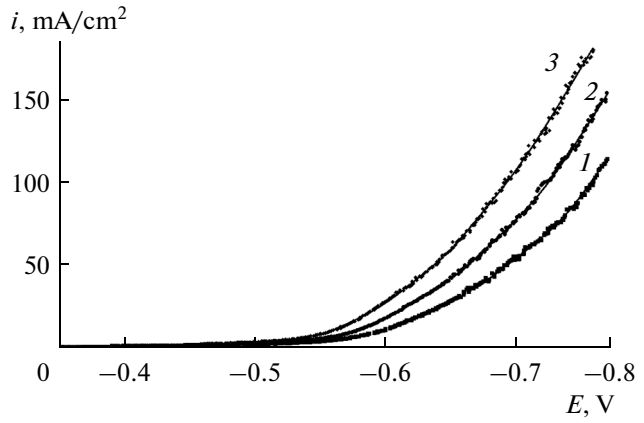

Fig. 2. Overall current density at the alloy deposition as a function of the cathode potential (NHE) at the temperature, °C: (*1*) 48, (*2*) 58, (*3*) 68.

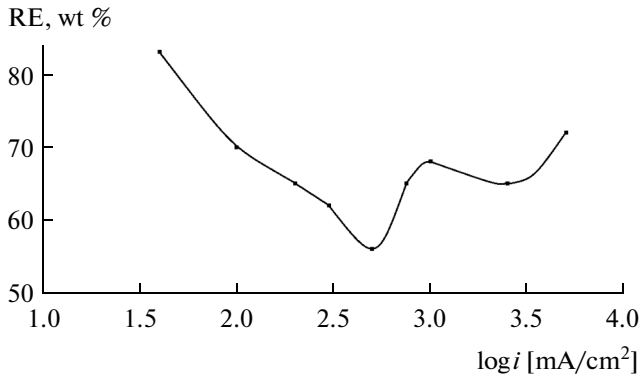

Fig. 3. Rhenium content in alloys as a function of the deposition current density.

esis. This may be associated with certain changes in the electrode surface structure and accumulation of hydrogen on the electrode surface, as confirmed by the considerable difference of open-circuit potentials (100–120 mV) before and after measuring polarization curves.

The high rate of hydrogen evolution and also the low CE of the alloy at the low current densities did not allow us to obtain partial polarization curves for the evolution of alloy components in this region; hence, the conclusions drawn should be considered as only preliminary. It cannot be ruled out that the shift of overall curves in the positive direction is also associated with the easier hydrogen evolution on the catalytically active surface (see Section 6).

3. Chemical Composition of the Alloy

Preliminary experiments have shown that the rhenium content in the deposits increases with the increase in solution acidity and the concentration of perrhenate. The dependence of nickel and rhenium contents in the alloys on the current density (calculated for the geometrical surface of the cathode was studied in a solution of the optimal composition in the interval of current densities of 0.04–5 A/cm^2. For the low current densities, the alloys contained mostly rhenium (Fig. 3); as the current density increased, its content decreased to reach minimum at the current density of 0.5 mA/cm^2 where the diffusion limitation with respect to nickel ions are substantial. Insignificant changes in the alloy composition (the increase in the rhenium content) observed at the higher current density (not shown in the figure) were probably associated with the increasing role of adsorbed hydrogen in the reduction of perrhenate ions and also with the decrease in the real current density as a result of electrode surface development at high current densities.

4. Phase Composition of the Alloy

Comparing the X-ray diffraction data with the results of chemical analysis of the alloy makes it possible to conclude that irrespective of its content in deposit, nickel is in the disordered state and does not form any individual phases. The nickel phase was present in the alloy only at extremely high current densities (5000 mA/cm^2). In all the cases, the strongly broadened rhenium reflex [101] was observed, i.e., the alloy lattice corresponded to the rhenium structure. The alloys in both compact and powder forms had the strongly disordered structure corresponding to the subgrain size of the order of magnitude of several nanometers (according to calculations, the lattice microdistortions could not lead to the observed broadening of X-ray diffraction peaks. As the temperature decreased, the complete amorphzation was observed. The rhenium lattice was considerably distorted as a result of incorporation of hydrogen and, probably, nickel; however, due to the strongly diffuse diffraction reflexes, we failed to determine accurately the changes in the average lattice period.

5. Hydrogen Content in the Alloys

The measurements of the hydrogen content carried out by the method of vacuum extraction have shown that the alloys contained from 1 to 7 cm^3 of hydrogen (per 1 g of alloy, recalculated to normal conditions). As the current density increased, the hydrogen content first somewhat decreased and then increased again (Fig. 4). The hydrogen content in the deposits prepared at 58°C passed through a minimum (1.3–1.4 cm^3/g) at 180–200 mA/cm^2 and then, at 100 mA/cm^2, increased to 3 cm^3/g and higher. The decrease in the solution temperature by 20°C resulted in a sharp increase in the hydrogen content in deposits and was accompanied by the complete conversion of deposits into the amorphous state. The hydrogen content found was slightly lower than that recently observed for Fe–Mo alloys [14].

By and large, the alloys containing more rhenium proved to sorb more hydrogen; however, their hydrogen content depended not only on the alloy composi-

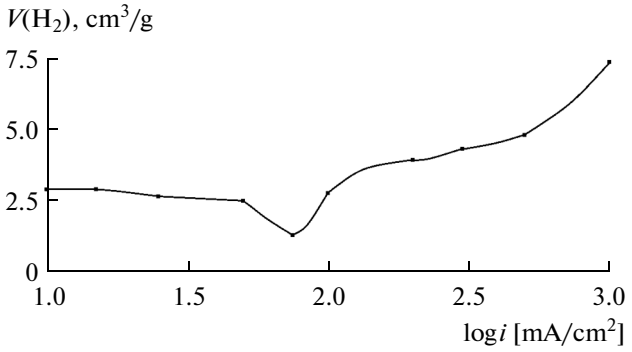

Fig. 4. Hydrogen content in alloys as a function of the deposition current density.

tion but also directly on the current density at the deposition, because the current efficiency with respect to hydrogen also changed. Due to the action of these two factors, as the cathodic potential increased, the overall rate of hydrogen evolution first decreased (due to the changes in the alloy composition) and then increased due to diffusion limitations with respect to metal ions. The dependence of the hydrogen content in deposits on the current density had the similar form.

6. Catalytic Properties of Nickel and Nickel–Rhenium Deposits in the Cathodic Hydrogen Evolution Reaction (HER)

The hydrogen evolution was studied in 0.1 M sulfuric acid solution on the surface of the alloy. For a comparison, the kinetics of this process was studied on a smooth platinum electrode (because the latter system is so well known, we studied our alloy in the same solution). The potential measurements were carried out in a three-electrode cell without any preliminary deep cleaning of electrodes (sulfuric acid solution of the reagent grade purity) and also in the cell thoroughly blown with argon and filled with electrolyte of the special degree of purity. A platinum rod served as the anode; a hydrogen electrode in the same solution served as the reference electrode. Before measuring voltammetric characteristics, the platinum working electrode was thoroughly cleaned by cycling its polarization in the anodic potential range. The true electrode surface area was determined by the charge of adsorbed hydrogen.

The nickel–rhenium alloy for this experimental series was deposited on a platinum wire with the diameter of 0.5 mm at the current density of 0.200 A/cm^2 (which corresponded to the beginning of dendrite formation so that the alloy composition under these electrolytic conditions corresponded to that of powders deposited in the current density range of 1–5 A/cm^2), and also on copper or nickel supports (we observed no effect of the support material on the electrocatalytic properties of the alloy).

The coating deposited on smooth platinum (the roughness factor was 1.2; this value was determined by comparing the geometrical surface of the electrode with the integral charge of adsorbed hydrogen, assuming that the latter is 210 μC/cm^2) was mirror bright which suggested that its roughness factor was also low.

According to preliminary experiments, the nickel–rhenium alloy exhibits the high electrocatalytic activity in HER exceeding in some cases the activity of smooth platinum. Figure 5 shows the results on the kinetics of hydrogen evolution on platinum and our alloy. The electrocatalytic activity of the smooth platinum electrode depended on the presence of impurities in electrolyte, particularly, chloride ions which strongly inhibited the HER. For nickel–rhenium electrodes, the Tafel slope was 80 mV per decade (this

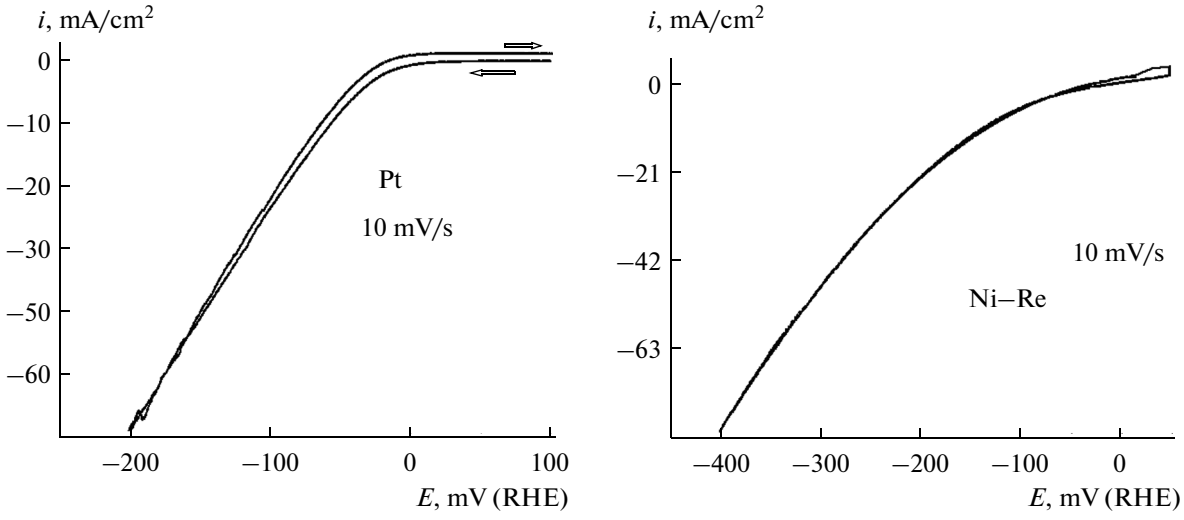

Fig. 5. Polarization curves of hydrogen evolution on platinum and Re–Ni alloy. Potential scan rate 10 mV/s. The potentials are recalculated to the scale of hydrogen electrode in the same solution.

is close to the value found in [15]) and the exchange current density of hydrogen was somewhat lower as compared with platinum electrode; however, no strong dependence of the HER overpotential on the electrolyte purity was observed. Hence, such electrodes can be used under far less clean conditions. Furthermore, it cannot be ruled out that under the conditions of hydrogen evolution in acidic media, the partial selective dissolution of nickel from the surface layer could occur, i.e., the surface could be enriched with rhenium.

The high catalytic activity of nickel–rhenium alloys can be explained, besides their high rhenium content, by the high degree of structural disordering.

ACKNOWLEDGEMENTS

This study was carried out with the financial support from the Russian Foundation for Basic Researches (project No. 11-03-00382).

REFERENCES

1. Woigt, F., *Trans. Amer. Electrochem. Soc.*, 1938, vol. 76, p. 635.
2. Fink, C.D. and Deren, P., *Trans. Amer. Electrochem. Soc.*, 1934, vol. 66, p. 472.
3. Suvorova, O.A. and Ippolitova, M.V., *Izv. AN Kaz. SSR, Ser. Metallurg.*, 1951, vol. 88, p. 56.
4. Pecherskaya, A.G. and Stender, V.V., *Zh. Fiz. Khim.*, 1950, vol. 21, p. 858.
5. Nezerton, L.E. and Holt, M.L., *J. Electrochem. Soc.*, 1949, vol. 95, p. 324.
6. Nezerton, L.E. and Holt, M.L., *J. Electrochem. Soc.*, 1951, vol. 97, p. 98.
7. Suvorova, O.A., *Doctoral (Chem.) Dissertation*, 1962.
8. Zabinski, P.R., Franczak, F., and Kowalik, R., *Arch. Metall. Mater.*, 2012, vol. 57, p. 495.
9. Naor, A., Eliaz, N., and Gileadi, E., *Electrochim. Acta*, 2009, vol. 54, p. 6028.
10. Berezina, S.I., Keshner, T.D., Khodyrev, Yu.P., and Veselkov, V.P., *Zashch. Met.*, 1993, vol. 29, p. 84.
11. Bus'ko, V.I., Gamburg, Yu.D., Zhulikov, V.V., and Konyukhov, V.Yu., *Korroz.: Mater., Zashch.*, 2013, no. 11, p. 1.
12. Zakharov, E.N. and Gamburg, Yu.D., *Russ. J. Electrochem.*, 2005, vol. 41, p. 892.
13. Esin, O.M., *Zh. Fiz. Khim.*, 1935, vol. 6, p. 795.
14. Kuznetsov, V.V., Golyanin, K.E., Pshenichkina, T.V., Lyakhov, B.F., and Lashenko, S.E., *Mendeleev Commun.*, 2013, vol. 23, p. 331.
15. Kuznetsov, V.A., Golyanin, K.E., Lyashenko, S.E., and Lyakhov, B.F., *Gal'vanotekh. Obrab. Poverkhn.*, 2013, vol. 21, no. 4, p. 18.

Translated by T. Safonova